Propylsulfonic and arenesulfonic functionalized SBA-15 silica as an efficient and reusable catalyst for the acidolysis of soybean oil with medium-chain fatty acids

Wenlei Xie *, Chi Zhang

School of Chemistry and Chemical Engineering, Henan University of Technology, Zhengzhou 450001, PR China

A B S T R A C T

The objective of this work was to develop a feasible ecofriendly process to produce medium-chain fatty acid (MCFA)-enriched structured lipids (SLs) in heterogeneous manners. For this purpose, the propyl-SO_3H or arene-SO_3H-modified SBA-15 materials were prepared through a surface functionalization of SBA-15 silica with propyl-SO_3H and arene-SO_3H groups. The organosulfonic acid-functionalized SBA-15 materials were characterized by Brönsted acidity determination, elemental analysis, XRD, C^{13} MAS NMR, FT-IR, SEM, TG, TEM, and N_2 adsorption-desorption techniques. Results showed that the propyl-SO_3H and arene-SO_3H groups were successfully tethered on the SBA-15 support, and the ordered mesoporous structure of SBA-15 silica was well retained after the organofunctionalization. This organic-inorganic hybrid material displayed high surface acidities and high activities in the acidolysis of soybean oil with caprylic or capric acid to produce SLs containing MCFAs. The influences of processing parameters on the reaction were investigated. The two studied catalysts showed an excellent recyclability for the reaction.

© 2016 Elsevier Ltd. All rights reserved.

1. Introduction

The physicochemical and functional properties of fats and oils are different according to the nature of fatty acids (FAs) on the glycerol backbone. Most natural vegetable oils offer limited applications in the edible oil industry when used in their unaltered form. The modification of vegetable oils can be employed as an efficient approach to enhance their functional performances targeting various commercial food applications (Xie & Zang, 2016). Structured triacylglycerols (TAGs) produced by combination of short-chain or medium-chain FAs with long-chain FAs are known as reduced-calorie or low-calorie structured lipids (SLs) (Zhao, Lu, Bie, Lu, & Liu, 2007; Zhang, Önal, Wijesundera, & Xu, 2009). Recently, these SLs have gained considerable attention since they can provide the physicochemical properties of fats with approximately half of the calories of typical edible oils. The presence of medium-chain fatty acids (MCFAs) and long-chain FAs in the same TAGs molecule will contribute to the unique nutritional and metabolic properties of these specialty lipids, which are rapidly oxidized as readily available energy, and generally are not accumulated in the adipose tissue (Nunes, Pires-Cabral, & Ferreira-Dias, 2011; Fomuso & Akoh, 2002). Such SLs can be usually produced by the acidolysis of vegetable oils, in which the MCFAs are incorporated into the TAGs. During the acidolysis processes, the acyl exchange of TAGs with FAs occurs, generating tailored TAGs and aiming at obtaining some desirable properties, such as reduced caloric value or modified melting point (Chnadhapuram & Sunkireddy, 2012; Mounika & Yella Reddy, 2012). In general, the acidolysis reaction is carried out by using lipase catalysts, either in solvent or in solvent-free media (Carrín & Crapiste, 2008; Hita et al., 2009). However, the application of enzymatic reactions is limited by the high cost associated with the lipase, the lack of long-term operational stabilities, and the difficulty in the recycling and reusing (Wang, Xia, Xu, Xie, & Duan, 2012). In this regard, from a practical application point of view, the development of a new type of efficient catalysts with a good stability for the acidolysis reactions have been an emergent and challenge field of scientific research.

Very recently, a green approach for chemical processes using sustainable heterogeneous acid catalysts has attracted significant attention. Heterogeneous catalysts possess several merits such as environmental friendly, easy separation from the reaction medium, and fewer disposal problems. Several heterogeneous acid catalysts,

---

* Corresponding author at: School of Chemistry and Chemical Engineering, Henan University of Technology, Zhengzhou 450001, PR China.
   E-mail address: xwenlei@163.com (W. Xie).

such as sulfated zirconia, tungstated zirconia, and sulfonated polystyrene compounds have been explored for the interesterification of vegetable oils (Garcia, Teixeira, Marciniuk, & Schuchardt, 2008; Park et al., 2010; Soldi, Oliveira, Ramos, & César-Oliveira, 2009). Until now, however to our knowledge, there is scarce report in the published literature regarding the solid acid catalysts used in the acidolysis of vegetable oils for the preparation of SLs (Xie & Hu, 2016). Accordingly, it is of much interest to fabricate the reusable, highly active and environmentally benign catalysts for the acidolysis reaction.

In the past decades, ordered mesoporous molecular sieves have been extensively investigated for their potential applications in many fields such as heterogeneous catalyst supports (Lebeau, Galarneau, & Linden, 2013). Among various mesoporous materials, SBA-15 silica is widely utilized as a promising support of heterogeneous catalysts, owing to their excellent structural properties, such as tunable pore size, large surface area, excellent stability, and facile functionalization with catalytically active groups (Zareyee, Asghari, & Khalilzadeh, 2011). Many efforts have been devoted to prepare SBA-15-type mesoporous materials that have large pore size and catalytic activities (Xie, Hu, & Yang, 2015). Recent studies have reported the incorporation of organosulfonic acid groups into mesostructured pore channels of mesoporous materials to introduce the catalytically organic acid sites (Shah, Parikh, & Maheria, 2014).The anchoring of organic acid moieties to silica surfaces by covalent bonds can produce the inorganic-organic hybrid nanocomposites with high Brönsted acid strength and plentiful numbers of acidic sites. Such hybrid nanocomposites can combine several advantageous aspects of both organic and inorganic species into mesoporous solids with the mechanical and reactive properties that are different from either of the wholly organic or inorganic component. Since the organic groups were covalently tethered onto the surface of the mesoporous support, the leaching of catalytically active groups can be expected to be avoided, thereby resulting in the improved activity of these inorganic-organic hybrid catalysts.

In continuing our development of heterogeneous catalysts for the modification of vegetable oils (Xie & Qi, 2013; Xie & Chen, 2014), the purpose of this current research was to prepare the organosulfonic acid supported SBA-15 catalysts, in which the organosulfonic acid was covalently anchored on the mesoporous SBA-15 silica, and then the formed solid acid catalyst was utilized to catalyze the acidolysis of soybean oil with MCFAs. Accordingly, the main novelty of this work lies in the use of the inorganic-organic hybrid material as an efficient and recyclable solid catalyst for the acidolysis reaction in a heterogeneous manner. Such hybrid mesoporous material can integrate the superiority of both homogeneous organic acid and heterogeneous catalyst, such as excellent catalytic efficiency and reusability, making it economic and environmentally preferable over the homogeneous catalyst. Here, soybean oil was used as reactants due to its high content of unsaturated FAs, mainly linoleic and linolenic acid. For the preparation of SLs containing MCFAs, caprylic and capric acids were also employed as acyl donors for the acidolysis reaction. Initially, a series of propylsulfonic or arenesulfonic acid functionalized SBA-15 materials was synthesized by grafting of propyl-SO₃H and arene-SO₃H groups onto the SBA-15 silica. These organosulfonic acid-functionalized SBA-15 nanocomposites were thoroughly characterized by means of Brönsted acidity determination, elemental analysis, small angle XRD, C¹³ MAS NMR, FT-IR, SEM, TG, TEM, and N₂ adsorption-desorption techniques. The influences of different acidolysis variables, including the substrate ratio, reaction time, catalyst loading, and reaction temperature on the incorporations of caprylic or capric acid were investigated systemically. Further, the stability and reusability of the solid acid catalysts were also evaluated in the present investigation.

2. Materials and methods

2.1. Materials

Refined soybean oil was purchased from local food store located in Zhengzhou, China. The acid value (AV) of the sampled oil was 0.082 mg KOH/g, which was determined by titration with a standard alkali solution. Tetraethylorthosilicate (TEOS, 98%), Pluronic P123 ($EO_{20}PO_{70}EO_{20}$, M_W = 5800), trimethoxyphenylsilane (TMPS, 98%) and (3-mercaptopropyl)trimethoxysilane (MPTMS, 98%) were purchased from Sigma-Aldrich. Caprylic acid (C8:0, ⩾98%) and capric acid (C10:0, ⩾98%) were also purchased from Sigma-Aldrich. All other chemicals were of commercially available analytical grade and used as received.

2.2. Catalyst preparation

The mesostructured SBA-15 silica was synthesized according to a hydrothermal method described previously (Srivastava, 2007).

The arenesulfonic acid modified SBA-15 silica was prepared as shown in Fig. 1. To functionalize the SBA-15 silica with arene-SO₃H groups, the trimethoxyphenylsilane was initially anchored onto the SBA-15 through covalent bonds affording phenyl SBA-15 silica (SBA-15-ph), and then the sulfonation of SBA-15-ph on the aromatic rings with chlorosulfonic acid was carried out so as to give the solid acid catalyst with a high surface area together with a large amount of surface —SO₃H groups. In a typical assay, a suspension of SBA-15 (1.0 g) and 3.0 g (15 mmol) of trimethoxyphenylsilane in 20 mL of dry toluene was refluxed for 24 h under nitrogen atmosphere. After this, the formed SBA-15-ph solid was separated by filtration, Soxhlet-extracted with toluene to remove the excess organosilane, and then vacuum-dried at 80 °C for 12 h. In the next step, 1.0 g of SBA-15-ph was suspended in 25 mL of dry 1,2-dichloroethane and refluxed under nitrogen atmosphere for 1 h. Thereafter, to the stirred solution of SBA-15-ph, 10 mL of chlorosulfonic acid as sulfonating agent was added dropwise, and subsequently the mixture was allowed to reflux with stirring for 5 h under nitrogen atmosphere. Finally, the functionalized SBA-15 silica was recovered by filtration, followed by washing with ethanol for several times. The so-prepared solid catalyst, designed as SBA-15-ph-SO₃H, was dried under vacuum at 80 °C for 10 h.

The propylsulfonic acid functionalized SBA-15 silica was synthesized following the procedure also described in Fig. 1. Typically, 1.0 g of dried SBA-15 and 3.0 g of 3-mercaptopropyltrimethoxysilane were added into 20 mL of dry toluene, and the resulting mixture was refluxed for 24 h under nitrogen atmosphere. Afterwards, the solids were filtered and washed successively with toluene and diethyl ether, after which they were subjected to Soxhlet extraction with CH₂Cl₂/Et₂O (1:1, by volume) mixture for 12 h to eliminate unreacted feedstocks, and then dried under reduced pressure at 80 °C. The produced mercaptopropyl functionalized SBA-15 (SBA-15-pro-SH) was oxidized by reaction with 30 mL of 30% H₂O₂ in 10 mL of methanol overnight at room temperature. The resultant solid was further acidified with 50 mL of 1 M H₂SO₄ solution, followed by washing with deionized water till the washings were neutral (Jin, Ansari, & Park, 2015). The obtained solid acid catalyst, denoted as SBA-15-pro-SO₃H, was finally dried under reduced pressure at 80 °C for 10 h.

2.3. Catalyst characterization

The Brönsted acid capacities of the inorganic-organic hybrid materials were determined by acid-base titration using NaCl solution as an ion-exchange agent (Amoozadeh & Rahmani, 2015).
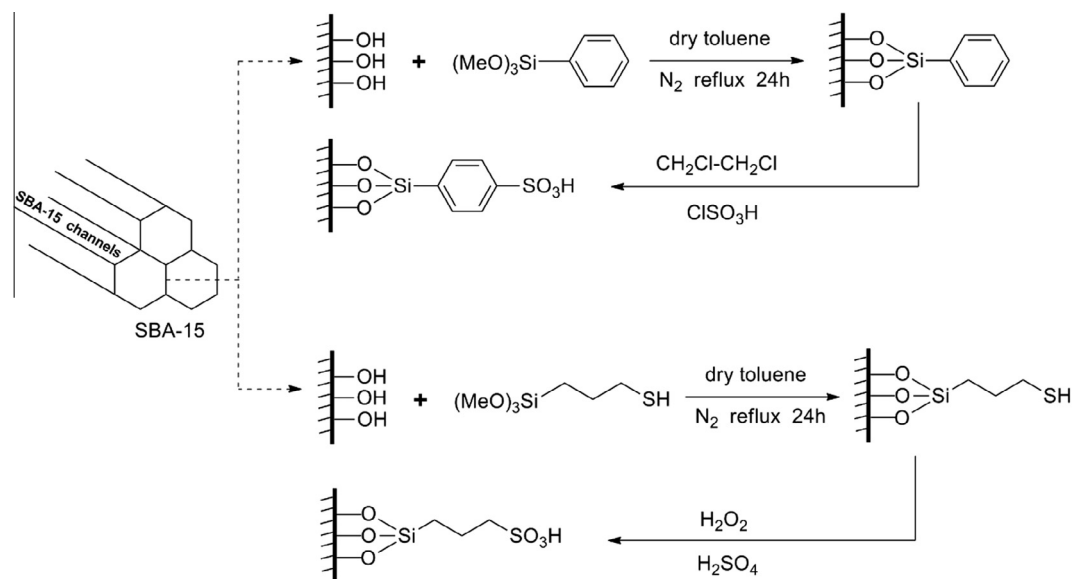
Fig. 1. Synthesis of SBA-15-ph-SO₃H and SBA-15-pro-SO₃H solid catalysts.

The carbon, hydrogen, and sulfur contents were determined with a Vario EL CUBE elemental analyzer. The amount of incorporated organosulfonic acid groups could be estimated according to the sulfur content of the solid catalysts. The N₂ adsorption-desorption isotherms were obtained by using a Quantachrome instrument (Model Nova 1000e series, Florida, USA) at liquid nitrogen temperature (−196 °C). The specific surface area, total pore volume, and mean pore diameter were assessed using the Brunauer-Emmett-Teller (BET) and Barrett-Joyner-Halenda (BJH) methods. Fourier transform infrared (FT-IR) spectra were recorded on a Shimadzu IR Prestige-21 spectrometer using KBr pressed powder discs. ^{13}C cross polarization (CP) magic angle spinning (MAS) nuclear magnetic resonance (NMR) spectroscopy of as-prepared samples was obtained on a Varian Infinity-plus400 spectrometer equipped with a 5 mm standard bore CP MAS probe head.

Thermogravimetric analysis (TG) was performed on a TA Instrument TG 2050 thermogravimetric analysis apparatus with a heating rate of 10 °C/min under air atmosphere. The small-angle XRD patterns were recorded on a Rigaku D/MAX-3B powder X-ray diffractometer using CuKα radiation. Scanning electron microscopy (SEM) was conducted on a field-emission microscope (JEOL, JSM-6390LV) operating at 15 kV. Transmission electron microscope (TEM) images were taken on a JSM-6390LV transmission electronic microscope.

2.4. Acidolysis procedures

Soybean oil (1.89 g) was mixed with caprylic (C8:0) and capric (C10:0) acid at different molar ratios in a 50 mL round-bottom flask fitted with a water-cooled condenser and a magnetic stirrer, and then the formulated blend samples were previously dried under reduced pressure at 80 °C for 1 h for removing moisture in the feedstocks. Thereafter, the appropriate amount of the solid catalyst was added into the reaction mixture. The acidolysis reactions were allowed to proceed under vigorously stirring at 160 °C with different substrate ratios. At the end of acidolysis, the reaction mixture was cooled to room temperature, and the solid catalyst was removed by filtration under reduced pressure. The acidolysis product was purified by alkaline deacidification to remove free FAs. To achieve this, the reaction mixture was dissolved in n-hexane, washed several times with 0.8 mol/L KOH solution (30% ethanol). The separated hexane phase (containing the TAGs) was further washed with 50% ethanol until it was neutral, and dried over anhydrous sodium sulphate. Finally, the hexane phase was evaporated under reduced pressure at 45 °C using a rotary evaporator, and the SLs containing MCFAs were thus obtained and the final product was employed for subsequent analysis.

All acidolysis reactions were performed in duplicate, and the incorporation of MCFAs was determined as the mass percentage of caprylic or capric acid in the TAGs of the produced SLs.

2.5. Analytical methods

FA compositions of the acidolysis products were determined after complete conversion of FA residues into their corresponding fatty acid methyl esters (FAMEs) by using KOH-methanol solution (2 mol/L) according to the AOCS method (AOCS, 2009). The FAMEs were analyzed on an Agilent gas chromatograph (model 6890N), fitted with a split injection port, a flame ionization detector, and data acquisition (Model Star Chromatography Workstation, version 5.5). Nitrogen was used as a carrier gas at flow rate of 1.2 mL/min with a split ratio of 1:20. The injector and detector temperatures were set at 260 °C and 300 °C, respectively. The initial temperature of the program was increased to 160 °C and then held for 5 min. This temperature was finally increased to 200 °C at a rate of 5 °C/min, and held isothermally for another 42 min at the final temperature. The FAMEs were identified by comparing their retention times of the peaks with the respective standards of FAMEs, and the FAME contents were obtained by area normalization and expressed as mass percentage

3. Results and discussion

3.1. Catalytic activity of the solid acid catalyst

The schematic pathways for the preparation of the solid acid catalysts are illustrated in Fig. 1. Firstly, the surface grafting technique was employed for incorporating organosilanes into the SBA-15 materials. Then, the modified SBA-15 material was further functionalized by sulfonation or oxidization reaction with the formation of the solid catalyst. The incorporation of organosulfonic acid groups into the SBA-15 material is an applicable approach to

prepare the organosulfonic acid functionalized silica catalyst. The arenesulfonic or alkylsulfonic acid functionalized mesoporous SBA-15 is the robust heterogeneous solid catalysts most likely due to their high Brönsted acid strength and plentiful numbers of efficient acidic sites that are favorable to the catalytic acidolysis reaction.

The total FA profile of soybean oil and acidolysis products is summarized in Table 1. As shown, the predominant FAs found in the soybean oil were linoleic acid (54.6%), followed by oleic acid (23.1%), palmitic acid (12.5%), linolenic acid (6.9%) and stearic acid (2.9%). After the catalytic acidolysis, the content of unsaturated FAs in the SLs was significantly decreased, whereas the caprylic and capric acid were found to be increased obviously, revealing that the solid catalysts can catalyze the incorporation of caprylic and capric acid into the soybean TAGs to give the MCFA-enriched SLs.

As expected, the unmodified SBA-15 displayed no considerable catalytic activity since the desired product was not obtained after 10 h of the reaction by using SBA-15 silica as a catalyst. The acid strength of the solid catalysts was estimated by the Hammet indicator method (Amoozadeh & Rahmani, 2015). The Hammett acidity function (H_0) of SBA-15-ph-SO$_3$H and SBA-15-pro-SO$_3$H catalysts was determined to be 0.88 and 1.08, respectively, showing that the two studied catalysts were strong solid acids. Mostly owing to this, both propyl-SO$_3$H and arene-SO$_3$H functionalized SBA-15 materials presented high catalytic activities to the acidolysis reaction, resulting in a large incorporation amount of caprylic and capric acid into the soybean TAGs over the two solid catalysts after 10 h of the reaction. Moreover, as compared with the propyl-SO$_3$H functionalized SBA-15, the arene-SO$_3$H functionalized SBA-15 silica with a phenyl group tethered to sulfonic acid groups exhibited higher acidolysis activities, because the higher incorporation levels of MCFAs were attained by using SBA-15-ph-SO$_3$H catalyst. This result may be due to more hydrophobic characteristic of phenyl group than that of propyl group, yielding local environments near the organosulfonic-acid active sites that are less sensitive to the poisoning effect of co-adsorbed water molecules.

In the present study, the SBA-15-ph-SO$_3$H catalyst was chosen for further study to optimize the preparation conditions. For this purpose, various SBA-15-ph-SO$_3$H catalysts with different loadings of arenesulfonic acids were prepared and tested for the acidolysis reaction, and the results are listed in Table 2. In this table, the loading of the arenesulfonic acid on the SBA-15 silica was determined from sulfur content by elemental analysis (mmol/g), assuming that all the sulfur elements are in the form of —SO$_3$H. The Brönsted acidity of the solid catalyst was defined as milliequivalents of acidic centers per gram of catalyst, and was determined by titration with standard NaOH solution. From the results displayed in Table 2, it was noticed that the Brönsted acidity present in the SBA-15-ph-SO$_3$H catalyst was very close to the loading amount of —SO$_3$H groups measured by elemental analysis, confirming that the acid capacity was mainly originated from the loaded arenesulfonic acid groups. Besides, with increasing TMPS amount from 3 to

15 mmol/g, the loading of arenesulfonic acid was increased gradually; simultaneously the Brönsted acidity together with the corresponding incorporation of MCFAs was also increased upon enhancing the arene-SO$_3$H group loading. However, as the TMPS amount was further increased beyond 15 mmol/g, there was no obvious increase in the loading amount of arene-SO$_3$H groups and the incorporation of MCFAs. In light of the results, the optimum amount of TMPS for the catalyst preparation was 15 mmol/g.

Lipase catalyst has been generally used to catalyze the acidolysis reaction, in which the triacylglycerols are firstly hydrolyzed into diacylglycerol and eventually monoacylglycerols, followed by the esterification of new FAs into the TAGs. In these two steps, acyl migration occurs, and accordingly byproducts such as diacylglycerols and monoacylglycerols are produced in the lipase-catalyzed acidolysis processes. However, by using the solid acid catalyst, different mechanisms were involved in the acid-catalyzed acidolysis reaction. As show in Fig. S1, Supplementary material, the carbonyl groups of the triacylglycerols are readily protonated by the solid acid catalyst, then attached by the carboxyl group of FAs, with the formation of a tetrahedral intermediate, as commonly occurs in the nucleophilic reactions of carboxylic acids (Parker & Baker, 1968). Thereafter, the acyl-oxygen cleavage occurs, thereby generating the SLs. From the viewpoint of mechanism, the diacylglycerols and monoacylglycerols cannot be formed in the acid-catalyzed processes. Moreover, to avoid hydrolysis reaction, free water was totally removed from the feedstocks under reduced pressure prior to the reaction. After the acidolysis reaction, the undesirable byproducts (monoacylglycerols and diacylglycerols) were not detected by TLC techniques.

3.2. Catalyst characterization

The incorporation of the organosulfonic acid groups in the mesoporous structure of SBA-15 silica was evidenced by FT-IR spectroscopy. Fig. 2A shows the FTIR spectra for SBA-15, SBA-15-ph, and SBA-15-ph-SO$_3$H sample. In the case of SBA-15 support, there were three characteristic Si—O—Si peaks centered at 1100 cm^{-1}, 770 cm^{-1}, and 450 cm^{-1}, which could be assignable to asymmetric stretching, symmetric stretching and bending vibration of the condensed silica network (Srivastava, 2007). Besides, the broad envelope peak located at about 3400 cm^{-1} for SBA-15 was largely ascribed to the surface OH stretching vibration, and the IR absorption peak at 967 cm^{-1} for the unmodified SBA-15 was attributed to the bending vibration of non-condensed Si—OH group in the SBA-15 material (Srivastava, 2007). For the SBA-15-ph sample, as comparison with the SBA-15 silica, the IR bands corresponding to surface OH groups (3400 cm^{-1} and 947 cm^{-1}) tended to reduce in intensity after the surface functionalization, indicating that the surface silanols are substituted by aminosilane groups. Meanwhile, after the organofunctionalization, the characteristic IR peaks resulting from the loaded organic groups were apparently observed as expected. For example, two weak IR absorption peaks at 3080 cm^{-1} and 3054 cm^{-1} corresponding to =CH stretching vibration of aromatic ring were observed for the SBA-15-ph sample, and three IR bands at 1572 cm^{-1}, 1480 cm^{-1}, and 560 cm^{-1} could be reasonably assigned to the aromatic ring absorption (Wang, Cheng, Chan, & Chao, 2006), thereby confirming the incorporation of phenyl group into the SBA-15 support. After the sulfonation reaction, the SBA-15-ph-SO$_3$H sample showed additional IR peaks at 654 cm^{-1} and 1172 cm^{-1}, which were tentatively assignable to C—S and O=S=O stretching mode vibrations, showing the presence of sulfonic acid groups on the SBA-15 (Amoozadeh & Rahmani, 2015). These results revealed that the successful incorporation of arene-SO$_3$H groups into the SBA-15 network with the formation of the SBA-15-ph-SO$_3$H catalyst.

Table 1
Total composition (wt.%) of FAs for soybean oil and acidolysis products after the reaction catalyzed by the two functionalized SBA-15 catalysts.

FA	C8:0	C10:0	C16:0	C18:0	C18:1	C18:2	C18:3
SO	0	0	12.5	2.9	23.1	54.6	6.9
After acidolysis (ph)[a]	38.3	42.2	3.3	0.8	6.3	9.1	0
After acidolysis (pro)[b]	30.2	30.8	10.4	3.1	11.7	13.1	0.7

[a] Catalyzed by SBA-15-ph-SO$_3$H, reaction conditions: C8:0/C10:0/SO molar ratio 5:5:1; catalyst loading 5 wt.%; reaction temperature 160 °C and reaction time 10 h.
[b] Catalyzed by SBA-15-pro-SO$_3$H, reaction conditions: C8:0/C10:0/SO molar ratio 6:6:1; catalyst loading 7 wt.%; reaction temperature 150 °C and reaction time 12 h.

Table 2
Catalytic activities, organosulfonic acid loading, acid capacity and textural properties of SBA-15-ph-SO₃H catalysts prepared with different TMPS amounts.[a]

TMPS/SBA-15 (mmol/g)	Loading amount (mmol/g)	Acid capacity (meq H⁺/g)	S_{BET} (m²/g)	V_p (cm³/g)	D_{BJH} (nm)	Incorporation of caprylic acid (mol%)	Incorporation of capric acid (mol%)
0[b]	–	0.05	744	0.97	7.14	Trace	Trace
3	0.40	0.36	682	0.89	6.97	7.3	12.0
6	0.54	0.50	675	0.86	6.64	16.8	22.1
9	0.82	0.76	608	0.79	6.01	30.5	35.7
12	1.04	0.95	562	0.76	5.63	36.2	39.4
15	1.153	1.09	545	0.71	5.35	38.3	42.2
18	1.165	1.11	542	0.70	5.23	37.9	42.5

[a] Reaction conditions: caprylic acid/capric acid/soybean oil molar ratio, 5:5:1; catalyst loading, 5 wt.%; reaction time, 10 h; reaction temperature, 160 °C.
[b] Pure SBA-15.
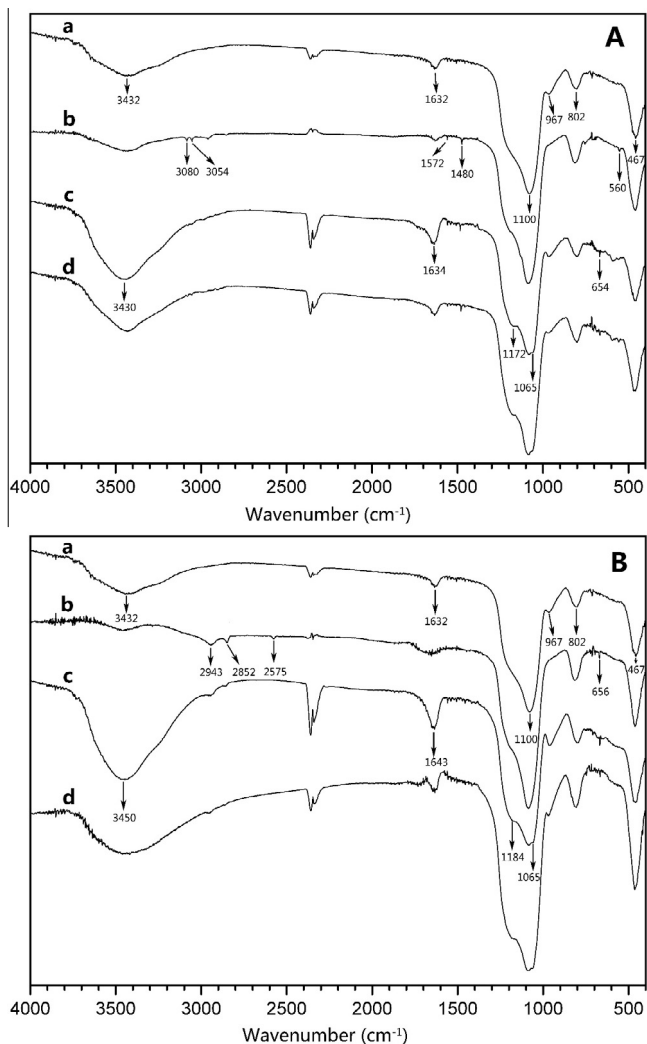
Fig. 2. FT-IR spectra of samples: A: (a) SBA-15; (b) SBA-15-ph; (c) SBA-15-ph-SO₃H; (d) used SBA-15-ph-SO₃H. B: (a) SBA-15; (b) SBA-15-pro-SH; (c) SBA-15-pro-SO₃H; (d) used SBA-15-pro-SO₃H.

In comparison with the SBA-15 silica, the SBA-15-pro-SH sample showed new IR absorption bands at 2943 cm⁻¹, 2852 cm⁻¹, and 2575 cm⁻¹ (Fig. 2B). The 2943 cm⁻¹ and 2852 cm⁻¹ bands were ascribed to the methylene C—H stretching vibration of propyl groups, while the IR band located at 2575 cm⁻¹ was attributable to the S–H stretching vibration, thus suggesting that the SBA-15 was virtually functionalized by the mercaptopropyl groups (Jin et al., 2015). However, after the oxidation with H₂O₂, the IR band at 2575 cm⁻¹ corresponding to S–H group was disappeared mostly

due to the total oxidation of —SH group into —SO₃H group. Moreover, the existence of sulfonic acid groups in the SBA-15-pro-SO₃H sample was also confirmed by the presence of characteristic IR bands of —SO₃H groups. For instance, for the SBA-15-pro-SO₃H sample, the IR bands at 3430 cm⁻¹ and 1634 cm⁻¹ were associated with S—OH stretching vibration, while the IR absorption peaks appeared at 1172 cm⁻¹ and 1065 cm⁻¹ were attributed to the O=S=O asymmetric and symmetric stretching vibration of —SO₃H group (Fig. 2B) (Amoozadeh & Rahmani, 2015). All these observations showed that the organosulfonic groups had indeed functionalized the SBA-15 support affording the SBA-15-pro-SO₃H catalyst.

For a further identification of anchored organosulfonic groups, ¹³C MAS NMR measurements were conducted over the organosulfonic acid functionalized SBA-15 samples, respectively. The ¹³C MAS NMR spectra of the two studied catalysts are displayed in Fig. S2, Supplementary material. In the solid NMR spectra, for the SBA-15-ph-SO₃H catalyst, three types of carbon species were assignable to arene-SO₃H groups: the resonance peaks at 141.7 ppm, 127.6 ppm and 148.3 ppm corresponded to ¹C, ²C and ³C carbon atoms, respectively (Wang et al., 2006). A weak resonance peak at 58.5 ppm was tentatively ascribed to carbon species of methoxy groups (Si—O—CH₃), originating from the incompletely hydrolyzed TMPS precursors (Jin et al., 2015). As for the SBA-15-pro-SO₃H sample (Fig. S2, Supplementary material), three ¹³C signals (11.4 ppm, 18.0 ppm and 53.8 ppm) were clearly seen as expected, which could be assigned to carbon species of Si—¹CH₂—²CH₂—³CH₂—SO₃H group (Wang et al., 2006). Overall, the NMR results further demonstrate that organosulfonic acid groups are practically incorporated into the parent SBA-15 silica.

The morphology and microstructure of SBA-15 and two functionalized SBA-15 materials were also characterized by SEM and TEM techniques. As observed in Fig. S3, Supplementary material, the parent SBA-15 was composed of well wheat-like macrostructures, which were aggregated with rope-shaped domains with relatively uniform particles around 1 μm, in agreement with the earlier literature (Srivastava, 2007; Xie et al., 2015). Moreover, the two functionalized SBA-15 samples showed a wheat-like morphology similar to the parent SBA-15. Obviously, no significant change in the surface morphology occurred after the surface organofunctionalization except that the domains were more densely packed. The representative TEM micrographs of the selected samples are shown in Fig. S4, Supplementary material. The SBA-15 and the two functionalized SBA-15 samples showed similar TEM images that displayed the presence of well-ordered regular arrays of one-dimensional channels with a mean diameter of about 6 nm and a wall thickness of around 3 nm, suggesting that the ordered mesoporous framework was essentially retained after the immobilization of organic moieties onto the siliceous SBA-15, in accordance with the results of other characterization techniques. Accordingly, it can be demonstrated that the grafting of organic functionalities does not destroy the mesoporous structure

of parent SBA-15, thus ensuring efficient reactant diffusion and catalytic acid sites accessibility during the acidolysis reaction.

The small-angle XRD patterns obtained for SBA-15 silica and two functionalized SBA-15 materials are presented in Fig. S5, Supplementary material. The SBA-15 sample exhibited three distinct XRD diffraction peaks at 0.91°, 1.56° and 1.76° in the low-angle region, which were indexed as (1 0 0), (1 1 0) and (2 0 0) planes of ordered mesoporous phase for the SBA-15 type material, respectively. This XRD pattern demonstrated typical two dimensional hexagonal p6 mm ordered mesostructure with a uniform mesoporous size distribution (Srivastava, 2007; Xie & Fan, 2014). Evidently, after the surface functionalization of SBA-15 silica, the two studied catalysts showed similar XRD patterns to the SBA-15 support, implying that the ordered mesoporous structure of SBA-15 silica was virtually retained even after the introduction of organic moieties into the SBA-15 silica, as also evidenced by the SEM and TEM techniques. Moreover, the (1 0 0) diffraction peaks for the two functionalized SBA-15 materials were shown to shift slightly to higher 2-theta values as compared to that of pure SBA-15 silica, indicative of the decrease of pore size upon the surface functionalization reaction (Zareyee et al., 2011). All the results suggested that the organofunctionalization process was successful and did not damage the pore structure of the SBA-15 materials.

The thermogravimetric plots for SBA-15-ph-SO_3H and SBA-15-pro-SO_3H samples are shown in Fig. S6, Supplementary material. For the two samples, there were two major mass loss regions in the TG curves. In the first region, a small amount of mass loss (4.5% for SBA-15-ph-SO_3H and 7% for SBA-15-pro-SO_3H) ranging from 25 °C to 150 °C with an endothermic event in the DTG curve, could be apparently attributed to the thermal removal of physisorbed water. It was noteworthy that the amount of adsorbed water for SBA-15-ph-SO_3H was less than that for SBA-15-pro-SO_3H, revealing that the former had lower surface hydrophilicity. With further increasing the temperature, a significant mass loss (about 18.3% for SBA-15-ph-SO_3H and 13.7% for SBA-15-pro-SO_3H), starting at 400 °C and finishing at 700 °C, and a strong endothermic event at about 500 °C were appeared. Considering the high endothermic temperature, this main mass loss could be principally ascribed to the thermal degradation of the functional groups attached on the SBA-15 framework. Above 700 °C, no obvious mass loss in the TG curve was observed for the two studied catalysts, indicating that the thermal decomposition of organic groups have completed at this temperature.

Fig. 3 depicts the N_2 adsorption-desorption isotherms and pore size distributions for SBA-15 silica and two functionalized SBA-15 materials. As can be seen, for all samples, the nitrogen adsorption isotherms were of type IV isotherms according to IUPAC classifications with a sharp capillary condensation step in the adsorption and desorption curve, and the isotherms displayed a pronounced steep H1 hysteresis loop at relative pressures in the range of 0.6–0.8, which were typical feature of ordered mesoporous materials with 2D hexagonal structure (Shah et al., 2014; Jin et al., 2015). Moreover, the amount of nitrogen adsorbed was decreased after the surface organofunctionalization, which may be caused by the presence of anchored organic moieties on the framework channel of the SBA-15 materials.

The textural properties of the two functionalized SBA-15 materials were investigated by nitrogen porosimetry measurements. As shown in Table 2, the SBA-15 silica was a porous material with a high surface area of 744 m^2/g and pore volume of 0.97 cm^3/g, while the mean pore size was calculated to be 7.14 nm, which are comparable to the literature value (Xie & Qi, 2013; Srivastava, 2007). In comparison with pure SBA-15, the BET surface area, pore diameter and pore volume of the functionalized SBA-15 materials were observed to decrease to some extent. This phenomenon suggested that the organosulfonic acid groups were loaded into the meso-
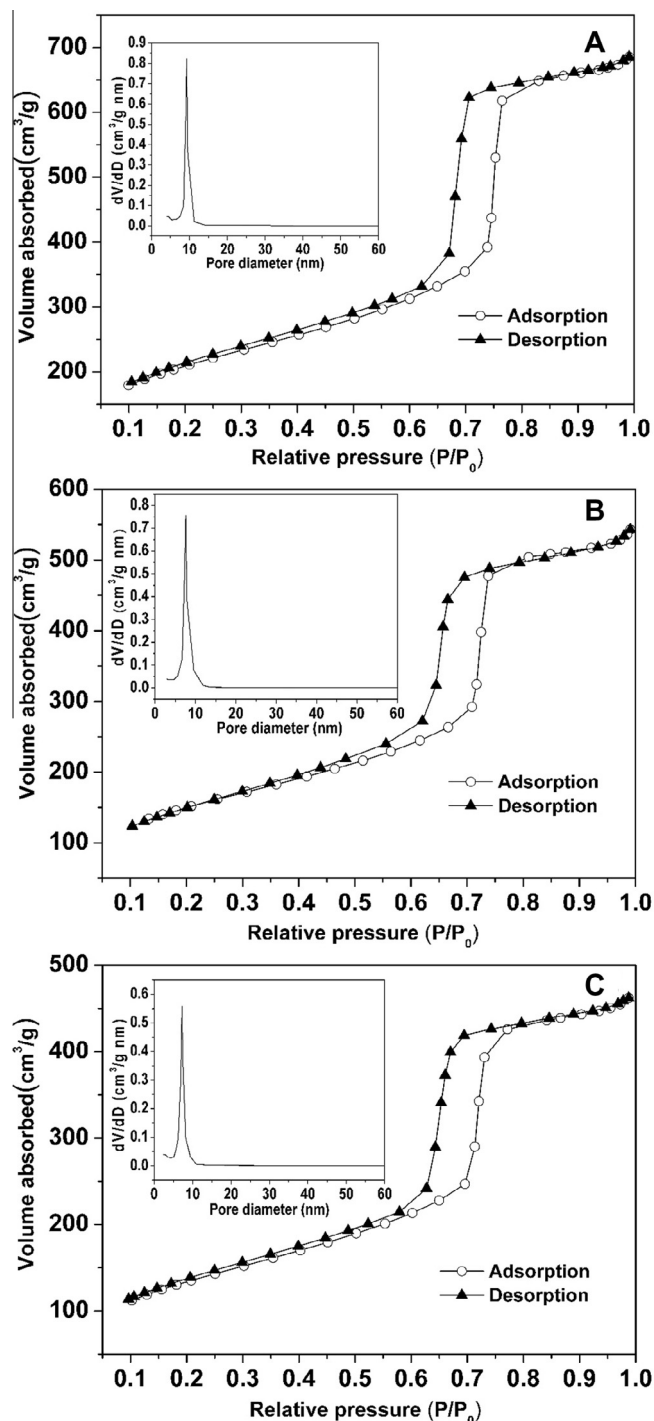

Fig. 3. Nitrogen adsorption-desorption isotherms and pore size distribution profiles (inset) of samples: (a) SBA; (b) SBA-15-ph-SO_3H; (c) SBA-15-pro-SO_3H.

porous structures of the SBA-15 support. Nevertheless, as observed from Table 2, the SBA-15-ph-SO_3H samples prepared with TMPS/ SBA-15 range of 3–18 mmol/g still possessed high surface area (682–542 m^2/g), large pore volume (0.89–0.71 cm^3/g) and narrowly distributed pores (6.97–5.23 nm). Therefore, the obtained inorganic-organic hybrid catalysts had long-range ordered mesostructure with relatively large surface area and high pore volume, which can increase the accessibility of catalytic sites to the feedsocks and facilitate the acidolysis reaction more rapidly. Besides, the ordered pore channel can decrease the mass transfer

limit of the reactants and products, allowing the reaction to be carried out easily.

3.3. Influence of reaction parameters on the acidolysis reaction

A preliminary screening of various acidolysis variables was performed to achieve the high corporations of the MCFAs, by using the two studied solid catalysts under heterogeneous conditions. The quantification of the incorporation amount of MCFAs in the soybean TAGs was performed by using GC methods. Based on the screening experiment results, to evaluate the effects of different parameters on the incorporation of caprylic or capric acids into SLs, the default reaction conditions were chose as the following: substrate mole ratio of 5:5:1 for SBA-15-ph-SO$_3$H catalyst and 6:6:1 for SBA-15-pro-SO$_3$H catalyst, reaction temperature of 160 °C for SBA-15-ph-SO$_3$H catalyst and 150 °C for SBA-15-pro-SO$_3$H catalyst, reaction duration of 10 h for SBA-15-ph-SO$_3$H catalyst and 12 h for SBA-15-pro-SO$_3$H catalyst, catalyst loading of 5 wt.% for SBA-15-ph-SO$_3$H catalyst and 7 wt.% for SBA-15-pro-SO$_3$H catalyst.

The influence of various reaction variables on the caprylic and capric acid incorporation was investigated for the optimization of the acidolysis process. The obtained results are illustrated in Figs. 4 and S7, Supplementary material. It can be seen from Fig. 4 that the incorporation values were always greater for capric acid than for caprylic acid for all the experiments by using SBA-15-ph-SO$_3$H as a catalyst under the same reaction conditions. This phenomenon showed that the incorporation of capric acid occurred more easily than that of caprylic acid, which was in agreement with the results

presented in previous literature (Chnadhapuram & Sunkireddy, 2012). However, over the SBA-15-pro-SO$_3$H catalyst, no obvious difference in the percentage incorporation between caprylic acid and capric acid was found in solvent-free media (Fig. S7, Supplementary material), in spite of using a series of experiments. Moreover, for the both selected MCFAs, higher incorporations were always attained by using SBA-15-ph-SO$_3$H catalyst as compared to SBA-15-pro-SO$_3$H catalyst, implying that the SBA-15-ph-SO$_3$H material had a higher catalytic activity to the acidolysis reaction.

The top left panel in Fig. 4 shows the incorporation values of MCFAs into soybean TAGs at various substrate molar ratios, as the SBA-15-ph-SO$_3$H catalyst was used for the acidolysis reaction. As could be seen, the extents of MCFA incorporations were considerably enhanced after 10 h of the reaction from 15.2 to 38.3% for caprylic acid and from 16.7 to 42.2% for capric acid by increasing the substrate molar ratio from 2:2:1 to 5:5:1. A higher caprylic or capric acid concentration of reaction mixtures favors the product formation by providing larger amounts of acyl groups during the acidolysis processes. The maximal incorporations for caprylic or capric acids were found at the caprylic acid/capric acid/ soybean oil molar ratio of 5:5:1. However, as the substrate ratio was further increased beyond 5:5:1, as indicated in Fig. 4, no significant change in the incorporations of caprylic or capric acid was observed. By using SBA-15-pro-SO$_3$H as a catalyst, as shown in Fig. S7, Supplementary material, a similar increase trend in the incorporations of MCFAs was observed. However, the maximal incorporation degrees over the SBA-15-pro-SO$_3$H catalyst for both caprylic and capric acid were achieved at the substrate ratio of 6:6:1.
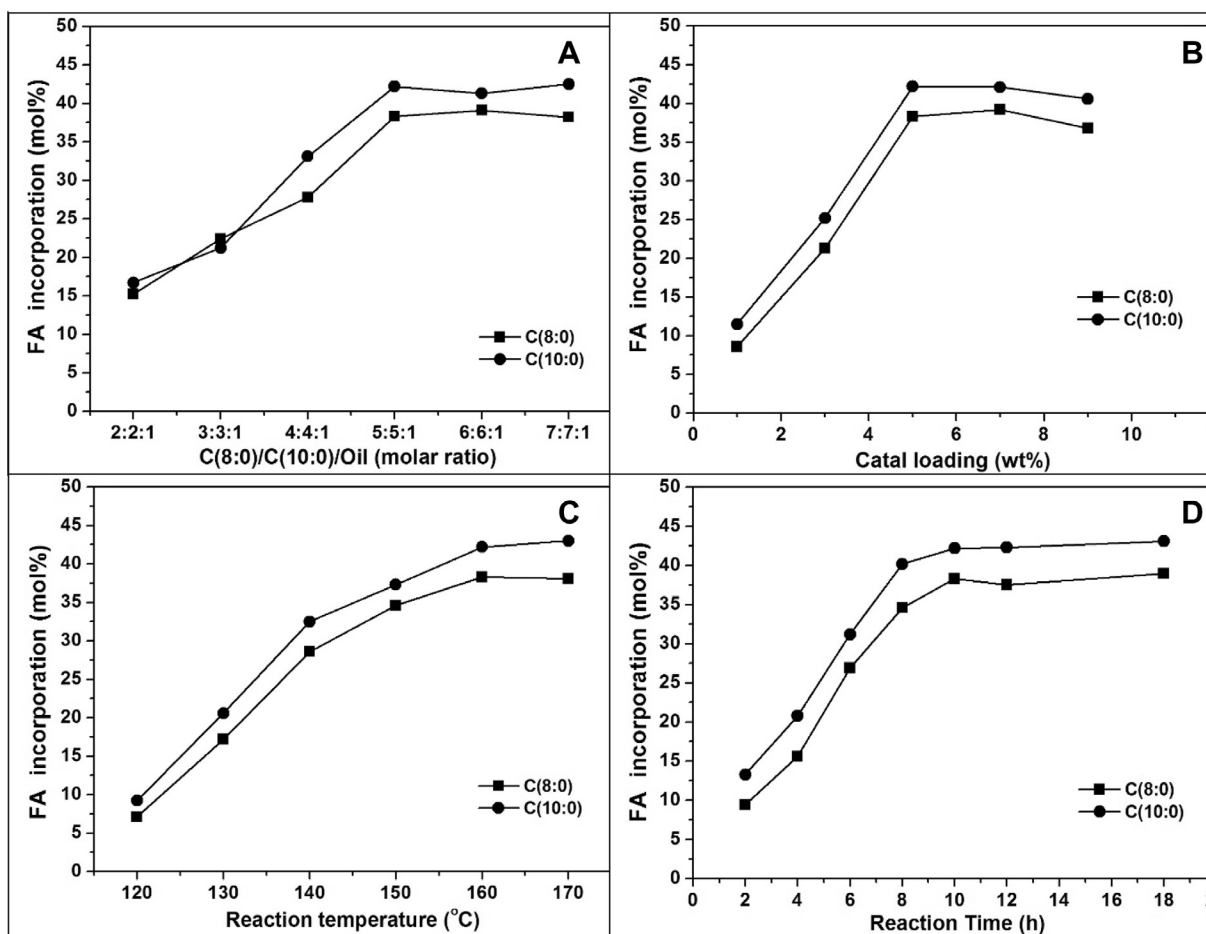

Fig. 4. Influence of acidolysis parameters on the incorporation of MCFAs into soybean oil over SBA-15-ph-SO$_3$H catalyst.

Several trials were conducted to elucidate the effect of catalyst loading on the incorporation of MCFAs at the substrate ratio of 5:5:1 with the SBA-15-ph-SO$_3$H catalyst, and the results are presented in the top right panel of Fig. 4. As expected, the acidolysis reaction did not proceed without the solid acid catalyst. As observed, when a low catalyst dosage of 1 wt.% was used, the obtained incorporations were only 8.6% for caprylic acid and 11.5% for capric acid, respectively, mostly due to insufficient catalytic sites to promote the acidolysis reaction. The MCFA incorporation over the SBA-15-ph-SO$_3$H catalyst was shown to increase steadily as the catalyst amount increased from 1 to 5 wt.%, and then the incorporation level was slightly declined with a further increase in catalyst loading beyond 5 wt.%. The highest incorporations for MCFAs were achieved at a catalyst loading of 5 wt.%. Generally, the increased catalyst loading enhances the availability of catalytically active sites and accordingly accelerates the acidolysis reaction rate, thus leading to the increased incorporations of acyl donors. However, a larger excess amount of catalyst may make the reaction mixture more viscous, thus increasing the mass transfer resistance in the heterogeneous system and thereby decreasing the incorporations of MCFAs. Therefore, the optimum catalyst loading for the reaction catalyzed by SBA-15-ph-SO$_3$H was considered to be around 5 wt.%. In the case of SBA-15-pro-SO$_3$H catalyst (Fig. S7, Supplementary material), the optimum catalyst loading was attained at 7 wt.%.

The plots of the percentage incorporation of the two MCFAs over the SBA-15-ph-SO$_3$H catalyst versus reaction temperature for the acidolysis reaction are given in the down left panel of Fig. 4. One can find that the reaction temperature has a significant impact on the acidolysis reaction. As can be seen, the percentage incorporations for caprylic and capric acid got increased after 10 h of the reaction as the reaction temperature rose from 120 °C to 160 °C. The optimum temperature for the acidolysis reaction was found to be 160 °C. At this temperature, the obtained incorporation degrees were 38.3% for caprylic acid and 42.2% for capric acid. However, with a further increase of reaction temperature beyond 160 °C, no obvious change in the incorporations for MCFAs was observed over the SBA-15-ph-SO$_3$H catalyst. Therefore, the suitable reaction temperature was set at 160 °C. For the SBA-15-pro-SO$_3$H catalyst, as indicated in Fig. S7, Supplementary material, similar results were obtained; however the maximal incorporation level was shown at 150 °C.

The effect of reaction time on the acidolysis reaction was also assessed within the time range of 2–18 h by using the SBA-15-ph-SO$_3$H catalyst. From the results displayed in downright panel of Fig. 4, it can be observed that the incorporation values for caprylic and capric acids were improved gradually with increasing the reaction time, reached a plateau value of 38.3% for caprylic acid and 42.2% for capric acid after 10 h of the reaction, and then remained almost constant thereafter, as a result of chemical equilibrium for the acidolysis reaction. Based on the results, the favorable reaction time was 10 h. For SBA-15-pro-SO$_3$H catalyst (Fig. S7, Supplementary material), a similar plot of reaction time against the incorporation value was obtained, and the optimum reaction time appeared at 12 h.

3.4. Reusability of the solid acid catalyst

The recycling of the solid catalyst after the reaction is critically required from the viewpoint of industrial application. For this purpose, after the acidolysis reaction, the used catalyst was recycled by filtration, following by washing with diethyl ether and methanol, and drying under reduced pressure overnight at 80 °C. After this treatment, the recovered catalyst was employed for the next reaction under the optimized reaction conditions. The obtained results are illustrated in Fig. S8, Supplementary material. As can

be seen, no significant loss in the catalytic activity was observed in the subsequent consecutive reuses for five cycles, revealing that the solid catalyst possesses excellent long-term stability. Moreover, the XRD pattern and FT-IR spectrum for the recovered catalyst were found not to be significantly varied when compared to the fresh one (Figs. 2 and S5, Supplementary material), which showed that the nature of the catalyst remained intact after the acidolysis process. The slight decrease in the catalytic activity may be reasonably ascribed to the accumulation of organic or carbonaceous materials on the mesoporous materials.

The heterogeneity of the solid catalyst was also verified by a leaching test. In the acidolysis process with the both MCFAs, the SBA-15-ph-SO$_3$H catalyst was removed from the reaction mixture after 6 h of the reaction through filtration (the incorporations of 26.9% for caprylic acid and 31.2% for capric acid at this time), and then the acidolysis was further continued for another 6 h at the same conditions without the catalyst. After further 6 h of the reaction, the incorporation levels for caprylic acid and for capric acid were just increased to 27.3% and 31.6%, respectively, confirming that the leaching of the acid species did not occur during the course of the acidolysis reaction. For the SBA-15-pro-SO$_3$H catalyst, similar results were also obtained (data not shown).

Therefore, the superiority of the sold acid catalysts lies in efficiently catalyzing the acidolysis of soybean oil to SLs containing MCFAs in a heterogeneous manner, taking advantages of easy recovery from the reaction mixture and then reuse for the new acidolysis reaction. To further evaluate the efficiency of the solid catalyst, more recently reported SBA-15-pr-NH$_2$-HPW catalyst by us was compared with the studied solid catalysts on the basis of the incorporations of MCFAs. Over the SBA-15-pr-NH$_2$-HPW catalyst that was prepared by the immobilization of phosphotungstic acid (HPW) on the amino-functionalized SBA-15 silica, the high incorporations of caprylic or capric acid of 58.7% or 61.9% was achieved, respectively, at 150 °C within 10 h when the two MCFAs were added individually as acyl donors. By using the SBA-15-ph-SO$_3$H and SBA-15-pro-SO$_3$H as a solid acid catalyst, the total incorporations for caprylic or capric acid of 80.5% and 61.4% were achieved after 10 h of the reaction at 150 °C, when the two MCFAs were added together into the reaction mixture. Clearly, the studied solid catalysts exhibited comparable activities to the already reported SBA-15-pr-NH$_2$-HPW catalyst.

4. Conclusions

The environmentally inorganic-organic hybrid acid catalysts, periodic ordered functionalized mesoporous SBA-15 materials bearing organosulfonic acid groups, were prepared by grafting of propyl-SO$_3$H and arene-SO$_3$H groups on the mesoporous SBA-15 silica. The catalyst characterization results showed that the propyl-SO$_3$H and arene-SO$_3$H groups were successfully tethered onto the SBA-15 silica with no damage in the ordered mesoporous structure of the SBA-15 silica even after the surface organofunctionalization. By using the solid catalysts, SLs containing MCFAs were prepared in an environmentally benign manner. It was demonstrated that the two studied solid catalysts not only exhibited high catalytic activities for the acidolysis of soybean oil but remarkably, they could be easily separated and reused with no significant loss of activity.

Appendix A. Supplementary data

Supplementary data associated with this article can be found, in the online version, at http://dx.doi.org/10.1016/j.foodchem.2016.05.025.

References

Amoozadeh, A., & Rahmani, S. (2015). Nano-WO$_3$-supported sulfonic acid: new, efficient and high reusable heterogeneous nano catalyst. *Journal of Molecular Catalysis A: Chemical, 396*, 96–107.

AOCS (2009). *AOCS official and recommended practices* (5th ed.). Champaign, IL, USA: AOCS Press.

Carrín, M. E., & Crapiste, G. H. (2008). Enzymatic acidolysis of sunflower oil with a palmitic-stearic acid mixture. *Journal of Food Engineering, 84*, 243–249.

Chnadhapuram, M., & Sunkireddy, Y. R. (2012). Preparation of palm olein enriched with medium chain fatty acids by lipase acidolysis. *Food Chemistry, 132*, 216–221.

Fomuso, L. B., & Akoh, C. C. (2002). Lipase-catalyzed acidolysis of olive oil and caprylic acid in a bench-scale packed bed bioreactor. *Food Research International, 35*, 15–21.

Garcia, C. M., Teixeira, S., Marciniuk, L. L., & Schuchardt, U. (2008). Transesterification of soybean oil catalyzed by sulfated zirconia. *Bioresource Technology, 99*, 6608–6613.

Hita, E., Robles, A., Camacho, B., González, P. A., Esteban, L., Jiménez, M. J., Muñío, M. M., et al. (2009). Production of structured triacylglycerols by acidolysis catalyzed by lipases immobilized in a packed bed reactor. *Biochemical Engineering Journal, 46*, 257–264.

Jin, H., Ansari, M. B., & Park, S. E. (2015). Sulfonic acid functionalized mesoporous ZSM-5: Synthesis, characterization and catalytic activity in acidic catalysis. *Catalysis Today, 245*, 116–121.

Lebeau, B., Galarneau, A., & Linden, M. (2013). Introduction for 20 years of research on ordered mesoporous materials. *Chemical Society Reviews, 42*, 3661–3662.

Mounika, C., & Yella Reddy, S. (2012). Specialty fats enriched with behenic and medium chain fatty acids from palm stearin by lipase acidolysis. *Journal of the American Oil Chemists' Society, 89*, 1691–1697.

Nunes, P. A., Pires-Cabral, P., & Ferreira-Dias, S. (2011). Production of olive oil enriched with medium chain fatty acids catalysed by commercial immobilised lipases. *Food Chemistry, 127*, 993–998.

Park, Y. M., Lee, J. Y., Chung, S. H., Park, I. S., Lee, S. Y., Kim, D. K., Lee, J. S., et al. (2010). Esterification of used vegetable oils using the heterogeneous WO$_3$/ZrO$_2$ catalyst for production of biodiesel. *Bioresource Technology, 101*, S59–S61.

Parker, V. D., & Baker, A. W. (1968). The mechanism of ester acidolysis. *Chemical Communications, 12*. 691-691.

Shah, K. A., Parikh, J. K., & Maheria, K. C. (2014). Biodiesel synthesis from acid oil over large pore sulfonic acid-modified mesostructured SBA-15: Process optimization and reaction kinetics. *Catalysis Today, 237*, 29–37.

Soldi, R. A., Oliveira, A. R. S., Ramos, L. P., & César-Oliveira, M. A. F. (2009). Soybean oil and beef tallow alcoholysis by acid heterogeneous catalysis. *Applied Catalysis A:General, 361*, 42–48.

Srivastava, R. (2007). An efficient, eco-friendly process for aldol and michael reactions of trimethylsilyl enolate over organic base-functionalized SBA-15 catalysts. *Journal of Molecular Catalysis A: Chemical, 264*, 146–152.

Wang, X., Cheng, S., Chan, J. C. C., & Chao, J. C. H. (2006). Template-free synthesis of mesoporous phenylsulfonic acid functionalized silica. *Microporous and Mesoporous Materials, 96*, 321–330.

Wang, Y., Xia, L., Xu, X., Xie, L., & Duan, Z. (2012). Lipase-catalyzed acidolysis of canola oil with caprylic acid to produce medium-, long- and medium-chain-type structured lipids. *Food and Bioproducts Processing, 90*, 707–712.

Xie, W., & Chen, J. (2014). Heterogeneous interesterification of triacylglycerols catalyzed by using potassium-doped alumina as a solid catalyst. *Journal of Agricultural and Food Chemistry, 62*, 10414–10421.

Xie, W., & Fan, M. (2014). Biodiesel production by transesterification using tetraalkylammonium hydroxides immobilized onto SBA-15 as a solid catalyst. *Chemical Engineering Journal, 239*, 60–67.

Xie, W., & Hu, P. (2016). Production of structured lipids containing medium-chain fatty acids by soybean oil acidolysis using SBA-15-pr-NH$_2$-HPW catalyst in a heterogeneous manner. *Organic Process Research and Development, 20*, 637–645.

Xie, W., Hu, L., & Yang, X. (2015). Basic ionic liquid supported on mesoporous SBA-15 silica as an efficient heterogeneous catalyst for biodiesel production. *Industrial and Engineering Chemistry Research, 54*, 1505–1512.

Xie, W., & Qi, C. (2013). Interesterification of soybean oil and lard blends catalyzed by SBA-15-pr-NR$_3$OH as a heterogeneous base catalyst. *Journal of Agricultural and Food Chemistry, 61*, 3373–3381.

Xie, W., & Zang, X. (2016). Immobilized lipase on core–shell structured Fe$_3$O$_4$-MCM-41 nanocomposites as a magnetically recyclable biocatalyst for interesterification of soybean oil and lard. *Food Chemistry, 194*, 1283–1292.

Zareyee, D., Asghari, R., & Khalilzadeh, M. A. (2011). Silylation of alcohols and phenols with hexamethyldisilazane over highly reusable propyl sulfonic acid functionalized nanostructured SBA-15. *Chinese Journal of Catalysis, 32*, 1864–1868.

Zhang, H., Önal, G., Wijesundera, C., & Xu, X. (2009). Practical synthesis of 1,3-oleoyl 2-docosahexaenoylglycerol by lipase-catalyzed reactions: An evaluation of different reaction routes. *Process Biochemistry, 44*, 534–539.

Zhao, H., Lu, Z., Bie, X., Lu, F., & Liu, Z. (2007). Lipase catalyzed acidolysis of lard with capric acid in organic solvent. *Journal of Food Engineering, 78*, 41–46.